Phase – Space Dynamics

Introduction

A mechanical system can be described completely by the Hamiltonian of the system $\boldsymbol{H(q,p,t)}$, where $\boldsymbol{q}$ is the generalized coordinates of the system and $\boldsymbol{p}$ is the generalized conjugate momenta of the system. The analysis of $\boldsymbol{q}$ with respect to time provides information regarding the path taken by the system but provides no information regarding the motion of the system. Conversely, analysis of $\boldsymbol{p}$ with respect to time reveals the time evolution of the momentum, and thus the energy of the system, but provides no information regarding the position of the system. Analysis of $\boldsymbol{p}$ with respect to $\boldsymbol{q}$ permits the examination of both position and momentum evolution of the system without explicit correspondence to time.

The analysis of $\boldsymbol{p}$ with respect to $\boldsymbol{q}$ is known as *phase-space dynamics* and involves expressing the Hamiltonian or equations of motion of the system of interest in terms of $\boldsymbol{p}$ and $\boldsymbol{q}$ only. The resulting equation can then be plotted in momentum-space to provide a visual representation of the system's behavior. One of the benefits of phase-space dynamics is that every phase-point on the phase-space plot represents the complete physical state of the system under consideration.

Application to Commonly-Encountered Systems

The concept of phase-space dynamics is most easily appreciated when applied to a few familiar systems:

Simple Pendulum

In this example, because the Hamiltonian is constant and equal to the energy of the system, the easiest way to generate a phase plot is to derive the Hamiltonian in terms of $\boldsymbol{p}$ and $\boldsymbol{q}$. The Hamiltonian of the simple pendulum illustrated in Figure 1, consisting of a mass m suspended by a massless string of length l is given by:

$$H(\theta,p) = T + V = \frac{p^2}{2ml^2} - mgl\cos\theta$$

In this particular case, it's obvious that $\theta = q$, the generalized coordinate and the Hamiltonian is timeindependent and is equal to the total energy of the pendulum system.

Figure 2 is the phase-space representation of the motion of the pendulum for four different values of the Hamiltonian or energy of the system. The innermost (green) curve or trajectory represents the motion of the pendulum for the lowest of the four energy levels. The pendulum has sufficient energy to swing through an angle of approximately $\pm\frac{\pi}{2}$ and obviously has the lowest maximum value of momentum. As time advances, the phase point representing the instantaneous state of the pendulum system repeatedly traces out the green trajectory, one period represented by a single orbit.

The blue trajectory represents the motion of the pendulum with slightly higher energy than the green trajectory as demonstrated by the higher maximum value for the momentum and θ.

The purple trajectory represents a higher energy than the blue or green and shows the swing angle θ approaching $\pm\pi$, the maximum swing angle while still retaining 'back and forth' motion. The orange, outermost trajectory represents the highest of the four energy levels and clearly demonstrates that the pendulum is now rotating continuously in one direction (no longer exhibiting 'back and forth' motion) by virtue of the open trajectory. An obvious implication of the open trajectory is that the system's momentum never falls to zero and continues in the same direction without limit.

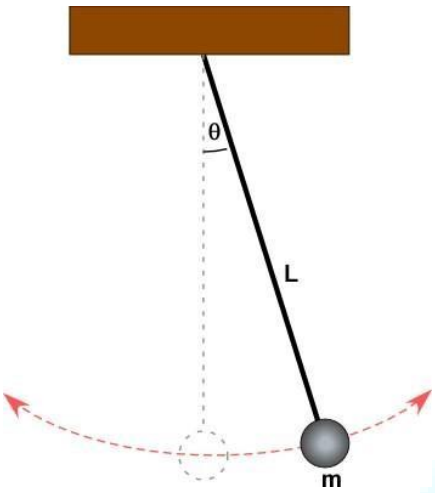

Figure 1: Simple pendulum

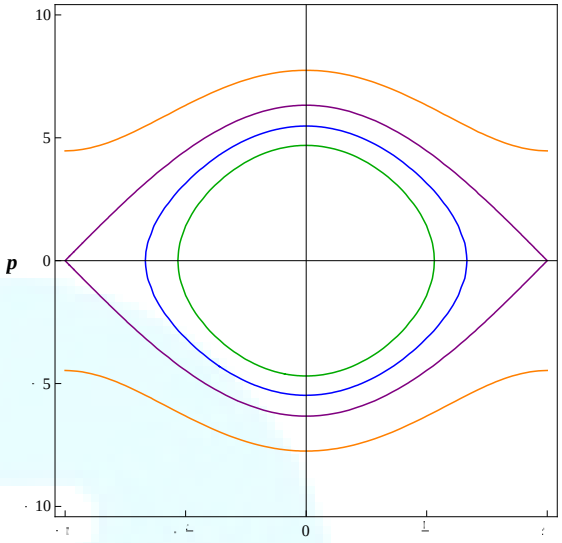

Figure 2: The simple pendulum represented in phase-space

Figure 3 shows this phase-space trajectory once more, but this time with q extended beyond the $\pm\pi$ limit of 'back and forth' motion.

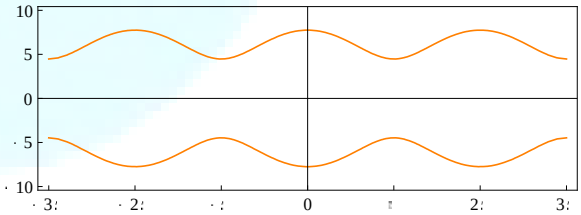

Figure 3: High-energy simple pendulum in phase-space

The phase-space trajectory that represents the motion of the pendulum at the limit where the p motion changes from 'back and forth' to continuous rotation is called the *separatrix*. The purple trajectory in figure 2 is very close in energy to the separatrix and is extremely close to it in q shape.

Damped Mass on a Spring

In this example, a mass m attached to the free end of a spring with spring constant k is subject to a damping force γ as shown in figure 4. A mass on an ideal spring exhibits simple harmonic oscillations and is described by the following differential equation:

$$m\frac{d^2x}{dt^2} + kx = 0$$

When the oscillations are subject to a damping force, the motion is described by:

$$m\frac{d^2\boldsymbol{x}}{dt^2} + \gamma\frac{d\boldsymbol{x}}{dt} + k\boldsymbol{x} = 0$$

Solving this differential equation provides us with the generalized coordinate $\boldsymbol{x}(t) = \boldsymbol{q}$. The generalized momentum can then be determined from the derivative of $\boldsymbol{x}(t)$.

$$\boldsymbol{p} = m\dot{\boldsymbol{x}}(t)$$

The obvious difference between this example and the simple pendulum is that $\boldsymbol{p}$ and $\boldsymbol{q}$ are both timedependent.
Solving the differential equation for the damped motion to find $\boldsymbol{q}$ and then differentiating to obtain $\boldsymbol{p}$, the phase-plot shown in figure 5 can be generated.

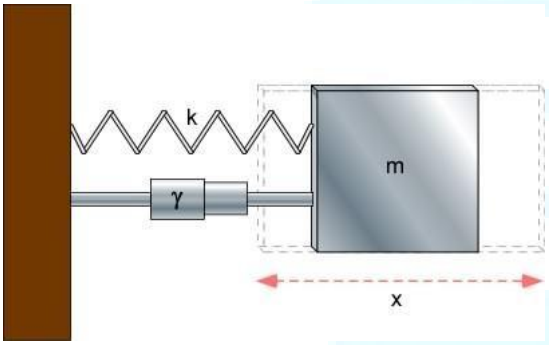

Figure 4: Damped mass on a spring

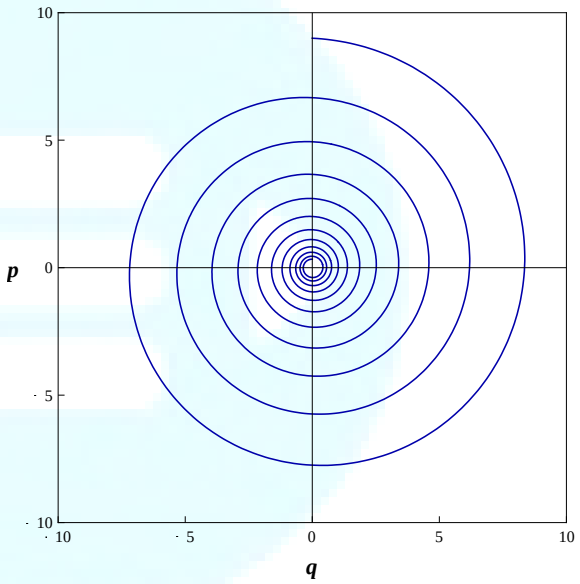

Figure 5: Phase plot of damped mass on a spring

The phase plot clearly shows how the momentum and displacement diminish with time resulting in a dramatic spiral trajectory. Without the damping force, the trajectory would be a closed ovoid similar to that for the simple pendulum with small oscillations. Figure 5 also shows how the damping force is reduced with diminishing momentum, a fact that is easily implied from the velocity term $\gamma\frac{d\boldsymbol{x}}{dt}$ of the differential equation .

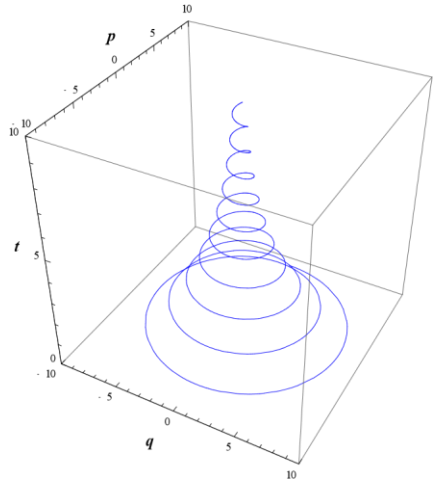

The time dependence of the phase-space trajectory of this system can be demonstrated even more dramatically with the use of a three-dimensional phase plot as shown in figure 6. In this plot, the vertical axis is time and the trajectory shows how the amplitude and momentum (and thus the energy) of the oscillations diminish rapidly at first, but more gradually as the oscillations become smaller and less energetic.

Figure 6: 3-D phase plot of damped mass on spring

Application to Complex Systems

While the relatively simple examples presented so far serve to introduce the concept and utility of phase-space dynamics, it's clear that many of the characteristics visually demonstrated in the phase plots are easily seen directly in the form of their differential equations. The true advantages of modeling dynamic systems in phase-space can be better appreciated when more complex systems are considered.

Forced Damped Harmonic Oscillator

This example starts from the differential equation that describes any simple harmonic oscillator, but with the addition of a damping force γ and a driving force with amplitude A and frequency ω:

$$m\frac{d^2\boldsymbol{x}}{dt^2} + \gamma\frac{d\boldsymbol{x}}{dt} + k\boldsymbol{x} = A\cos(\omega t)$$

With the behavior of the system now being influenced by five parameters, there are a tremendous number of states of the system that can be analyzed in phase-space.

No Damping:

With $\gamma = 0$ (no damping) and $A = 0$ (no driving force), it's obvious that we can recreate the ovoid phase plots produced for the ideal pendulum and a variety of other ideal oscillatory systems. As we start to apply a driving force, a steady state is reached immediately where the motion of the system results from the combination of the natural frequency and the forcing frequency. When the ratio of the natural frequency to the forcing frequency is an integer or a reciprocal integer, the phase-space trajectory demonstrates beat frequencies of the system in a very distinctive way (see figures 7 and 8).

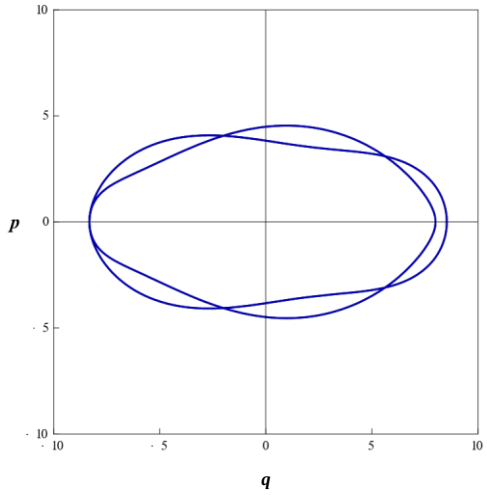

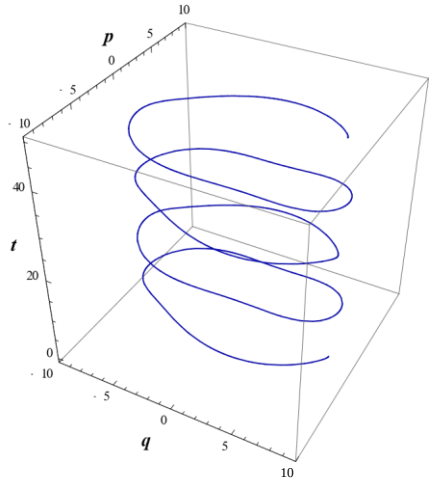

Figure 7: Driven SHO, integer relationship between natural frequency and driving frequency.

Figure 8: Driven SHO, integer relationship between natural frequency and driving frequency.

$$m = 4 \quad k = 1 \quad \gamma = 0 \quad A = 3 \quad \omega = 1.75$$

Under-damped:

With a small amount of damping and a relatively large spring constant ($\gamma < \sqrt{k}$), the phase plot shows that the initial transient motion of the system is a neat spiral trajectory. The trajectory reaches a steady state when the system is oscillating at the forcing frequency, indicated on the phase plot as the central ovoid (see figures 9 and 10). This phase-space trajectory is similar to the damped mass spring system except that the oscillations don't diminish in amplitude completely.

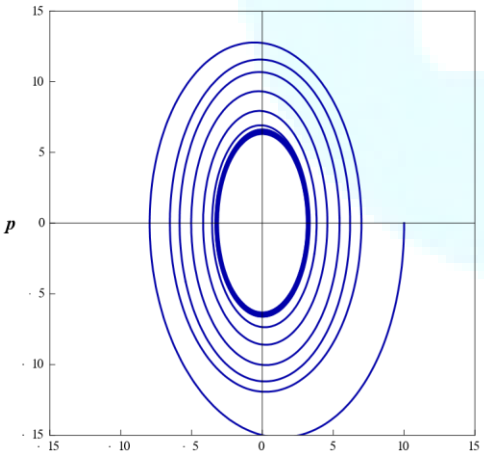

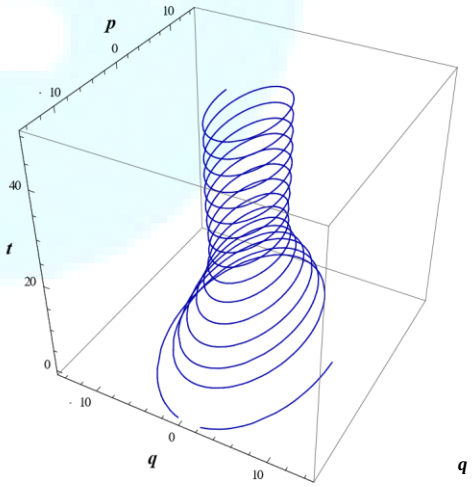

Figure 9: Driven, under-damped SHO stabilizes at driven frequency.

Figure 10: Driven, under-damped SHO stabilizes at driven frequency.

$$m = 3 \quad k = 10 \quad \gamma = 1 \quad A = 10 \quad \omega = 2$$

Over-damped:

A large damping force eliminates any periodicity in the initial transient motion of the system, but eventually a steady state is reached as with the under-damped case. The limiting orbit reached after the initial transient motion is called the *limit cycle* and, as stated in the under-damped case, has the same period as the driving force.

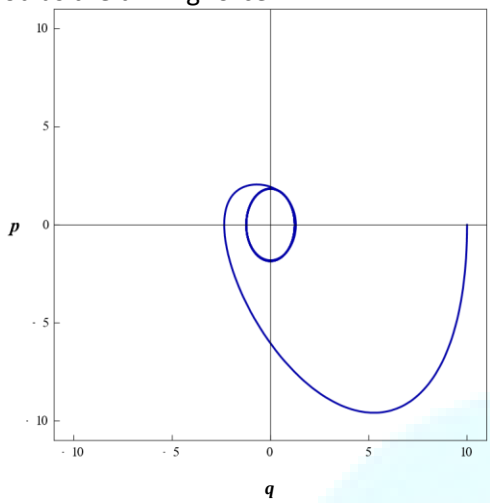

Figure 11: Driven, over-damped SHO stabilizes at driven frequency.

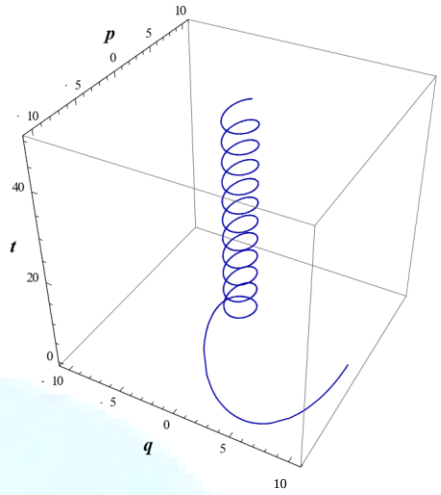

Figure 12: Driven, over-damped SHO stabilizes at driven frequency.

$$m = 3 \quad k = 10 \quad \gamma = 5 \quad A = 10 \quad \omega = 1.5$$

Resonance:

Limit cycle amplitude reaches a maximum at resonance (natural frequency = driving frequency). With light damping, even with the initial position set to zero (all previous examples have initial position $q \cong 10$), the phase plot amplitude grows rapidly and produces an impressive outward spiraling trajectory shown in figures 13 and 14. The trajectory shown has not reached the limit cycle yet. Given enough time, the trajectory will continue to spiral out until the limit cycle is reached. Figures 15 and 16 show the phase plot for the same resonance conditions, except for an increase in damping and an increase in the run time in order that sufficient time is provided for the steady state to be reached.

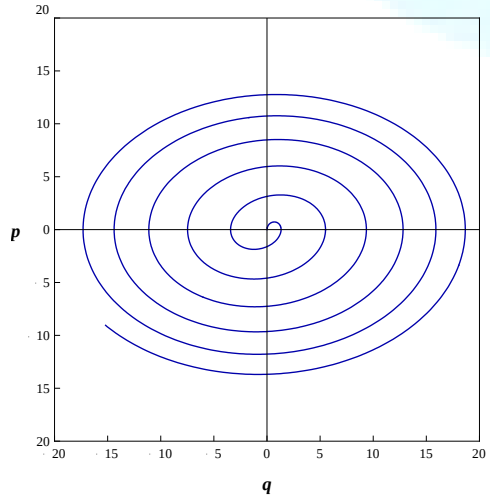

Figure 13: Driven, damped SHO at resonance. Initial transient motion only

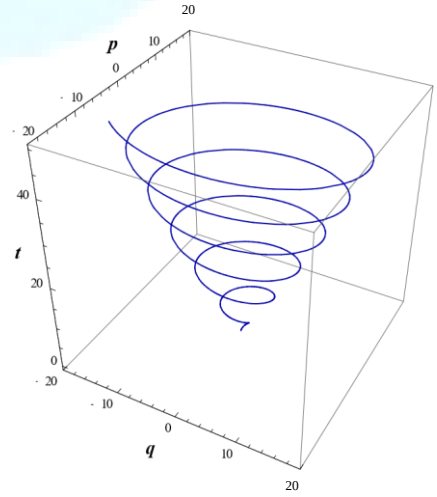

Figure 14: Driven, damped SHO at resonance. Initial transient motion only.

$m = 4 \quad k = 2 \quad \gamma = 0.1 \quad A = 3 \quad \omega = 0.71 \quad initial\ q = 0$

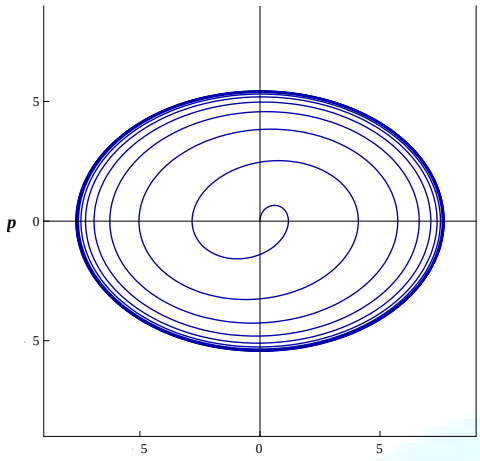

Figure 15: Driven, damped SHO at resonance. Given enough time to reach limit cycle.

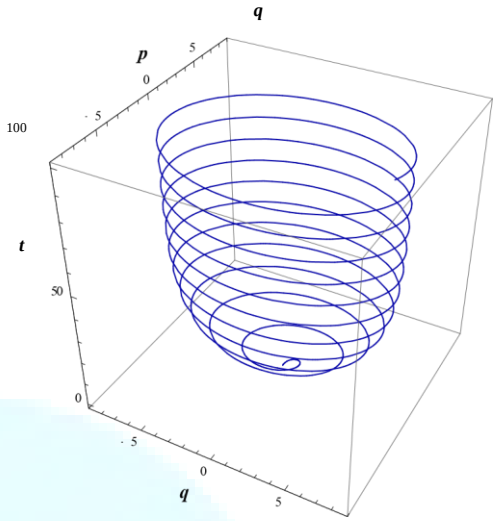

Figure 16: Driven, damped SHO at resonance. Given enough time to reach limit cycle.

$m = 4 \quad k = 2 \quad \gamma = 0.55 \quad A = 3 \quad \omega = 0.71 \quad initial\ q = 0$

Transient behavior:

The resonance case examined above gives an indication that the initial transient behavior of the system can be more interesting in phase-space than the steady state. Initial transient behavior results from different combinations of the natural frequency of the system and the driving frequency and minimal damping can cause the initial transient behavior to last for a long time before steady state is attained. The apparent struggle between the driving frequency and the natural frequency of the system can produce some bizarre phase plot trajectories that can resemble chaotic motion.

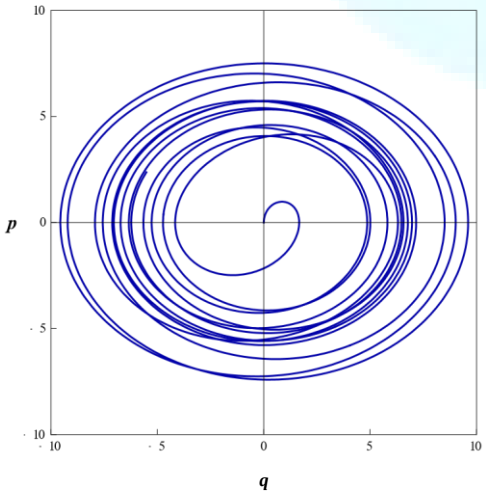

Figure 17: Transient behavior.

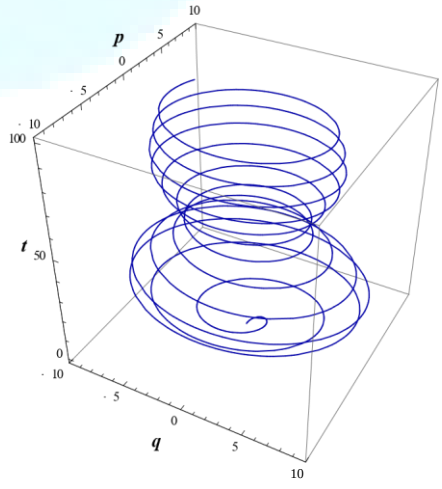

Figure 18: Nice vase!

$m = 4 \quad k = 2 \quad \gamma = 0.2 \quad A = 4.5 \quad \omega = 0.82 \quad initial\ q = 0$

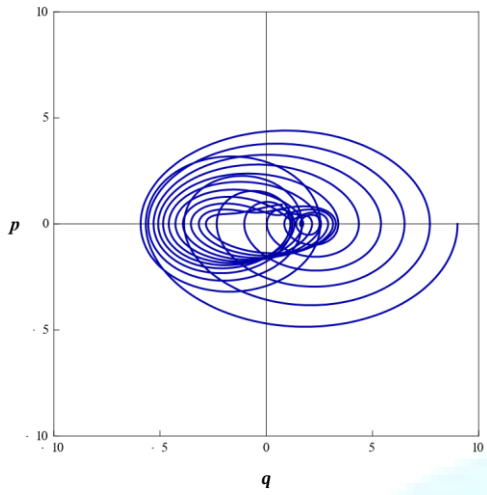

Figure 19: Transient behavior.

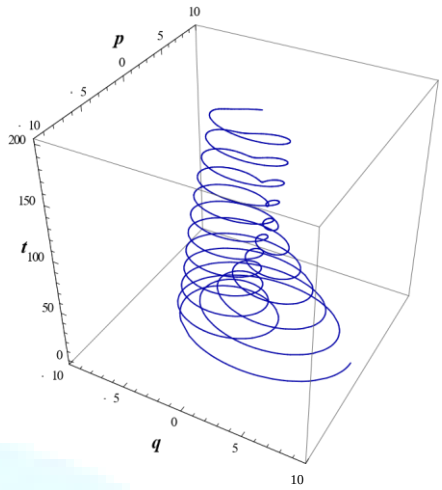

Figure 20: Transient behavior.

$$m = 4 \quad k = 2 \quad \gamma = 0.1 \quad A = 4.5 \quad \omega = 0.34 \quad initial\ q = 9$$

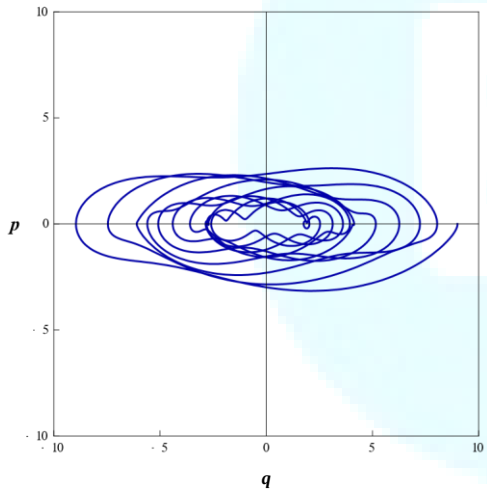

Figure 21: Transient behavior.

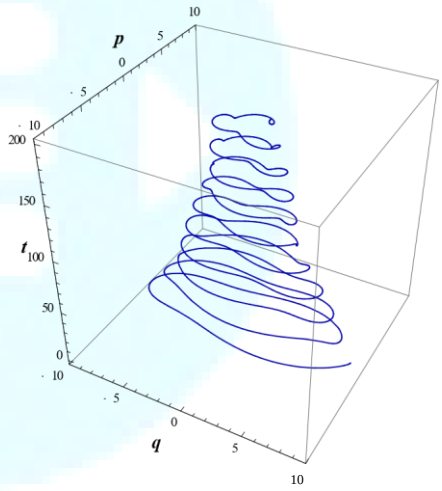

Figure 22: Transient behavior.

$$m = 10 \quad k = 1 \quad \gamma = 0.15 \quad A = 4.5 \quad \omega = 1.2$$

Infinite possibilities:

The Mathematica '*Manipulate*' feature was used with '*ParametricPlot*' and '*ParametricPlot3D*' to interactively adjust the five parameters (m, k, γ, A, ω) and to automatically produce the above phase plots. Additionally, the initial position of the system, the length of time the system is allowed to run and zoom in and out are adjustable. The Mathematica notebook accompanying this work contains this tool and the reader is strongly encouraged to experiment further with it, since there are many more combinations of parameters that yield fascinating and unexpectedly informative phase-space trajectories.

Charged Particles in a Quadrupole Field

Figure 23: Four rod electrode arrangement commonly used to produce a quadrupole field.

Quadrupole electric fields are commonly employed in mass spectrometric and associated instrumentation. The name *quadrupole* derives from the four-fold symmetrical nature of the electric field generated when a specific combination of DC and radio-frequency AC voltages are applied to symmetrically arranged electrodes. The most common electrode arrangement is that of four rods as shown in figure 23, but a number of other electrode arrangements are also used.

The behavior of charged particles such as ions in a quadrupole field is derived from the *Mathieu equation* (Dawson, 1976):

$$\frac{d^2y}{dx^2} + (a - 2q\ \cos(2x))y = 0$$

Emile Mathieu introduced this differential equation as a means to represent the motion of elliptical drumheads, but the equation has since been applied to many other problems.

One of the forms of this equation appropriate for the application at hand is one concerning the radial motion of a singly-charged ion in a quadrupole field (Dawson, 1976) (Lichtenberg, 1969):

$$\frac{d^2r}{dx^2} + \frac{e}{m\,r_0^2}(U - V\ \cos(\omega t))r = 0$$

The parameter U is the DC voltage component applied to the electrodes and V is the amplitude of the radio-frequency AC voltage component applied to the electrodes with frequency ω. r_0^2 is the initial radial position of the ion as it enters the quadrupole field and, as will become clear later, is particularly important in this application. Our generalized coordinate in this case is of course r and, as before, the ion's momentum is found from the derivative of the solution to the differential equation above. Once again, with five adjustable parameters, analyzing the motion of just a single ion is tremendously complicated. However, as we examine just a few phase plots of the ion's radial motion, it's important to realize that as the ion enters the quadrupole field, it has a relatively small velocity perpendicular to r (imagine the ion moving from left to right, close to and parallel to the centerline of the electrodes). As the ion traverses the length of the quadrupole field, if its radial displacement becomes too large, it will collide with one of the electrodes and most likely become neutralized by gaining an electron from the electrode's metallic surface. Only ions that attain and maintain a small relatively stable oscillatory phase-space trajectory will traverse the full length of the quadrupole field. This of course, is the principle behind the *quadrupole mass filter* (QMF) that is employed in many mass spectrometers.

Stable trajectory – ion passes through the field:

Figures 24 and 25 show the phase plots for an ion that quickly establishes a stable oscillatory trajectory and maintains it through the period of time that it would travel through the full length of the quadrupole field.

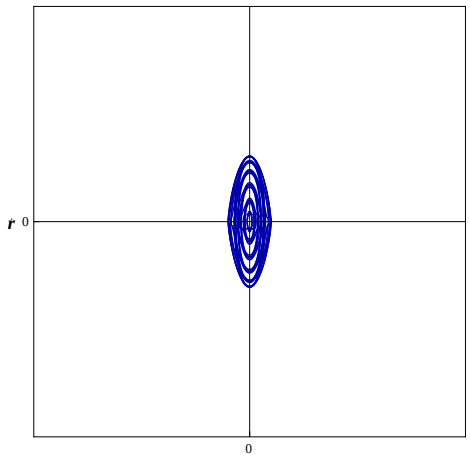

$m = 30 \quad U = 3 \quad V = 3 \quad \omega = 2.55 \quad r_0 = 0.1$

Figure 24: Stable ion trajectory.

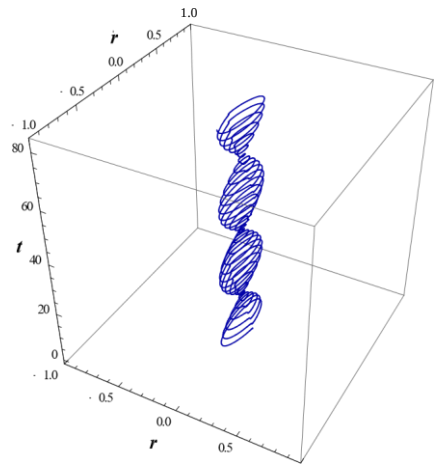

Figure 25: Stable ion trajectory.

The accompanying Mathematica file contains the tool that was used to create these phase plots and again, the reader is encouraged to manipulate the parameters to observe the effects on the ion's trajectory. In particular, the frequency of the RF voltage has a dramatic effect and it can easily be seem how a range of masses can be selected using a quadrupole mass filter of this sort.

Unstable trajectory – ion ejected from the field:

Figures 26, 27, 28 and 29 show phase plots of ions with unstable trajectories. Soon after entering the quadrupole field, the displacements of the ion increase rapidly and they would certainly impact an electrode surface and be neutralized.

Notice that the only difference in the parameters between figures 24 and 25 and those for figures 26 and 27 is just the small change in the RF frequency ω. Figures 28 and 29 demonstrate some pretty dramatic effects for low values of ω.

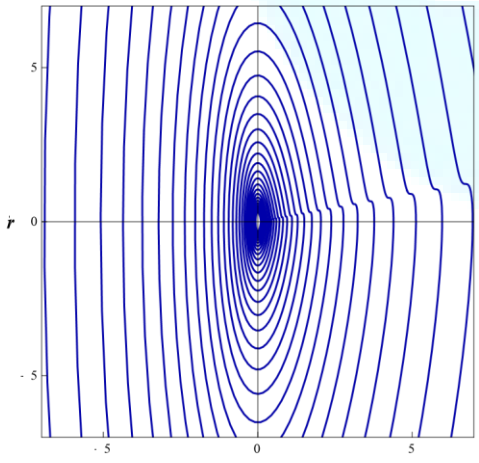

Figure 26: Unstable ion trajectory.

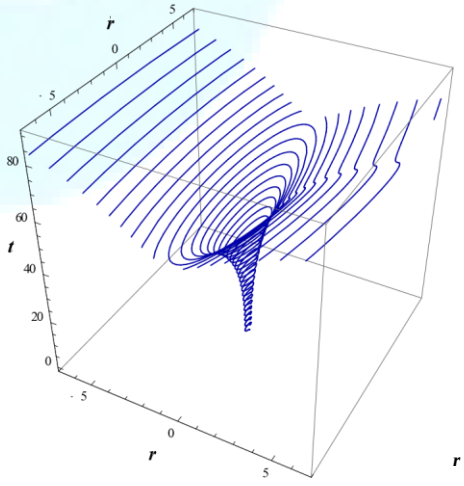

Figure 27: Unstable ion trajectory.

$m = 30 \quad U = 3 \quad V = 3 \quad \omega = 2.55 \quad r_0 = 0.1$

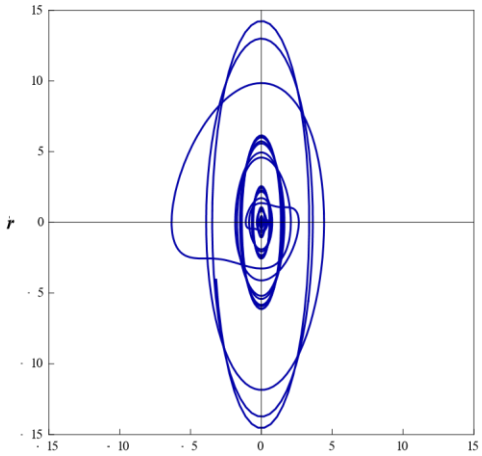

Figure 28: Unstable ion trajectory.

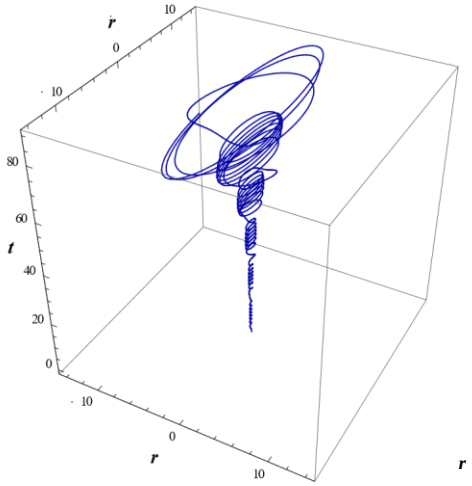

Figure 29: Unstable ion trajectory.

$$m = 30 \quad U = 3 \quad V = 3 \quad \omega = 0.38 \quad r_0 = 0.1$$

Dependence on the ion's initial position:

The previous cases have clearly demonstrated how sensitive the ion's trajectory is to changes in ω and it stands to reason that the exact point of entry into the quadrupole field will have a significant effect on the trajectory also. This is obvious from examining the governing differential equation that has a $1/r_0^2$ term multiplying both the DC and the AC voltage terms.

Figures 30 and 31 were generated from another plotting tool from the accompanying Mathematica file and involve the trajectories of three identical ions entering the quadrupole field in different places superimposed on the same plot.

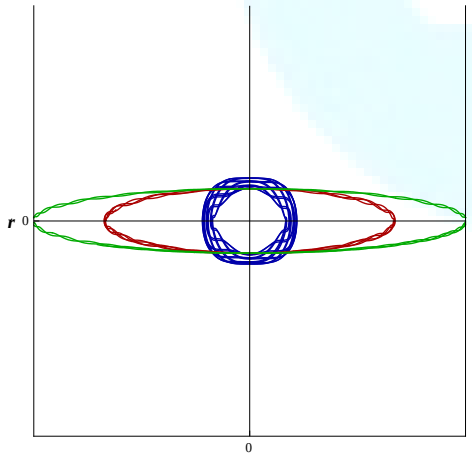

Figure 30: Trajectories for three identical ions initial radial positions.

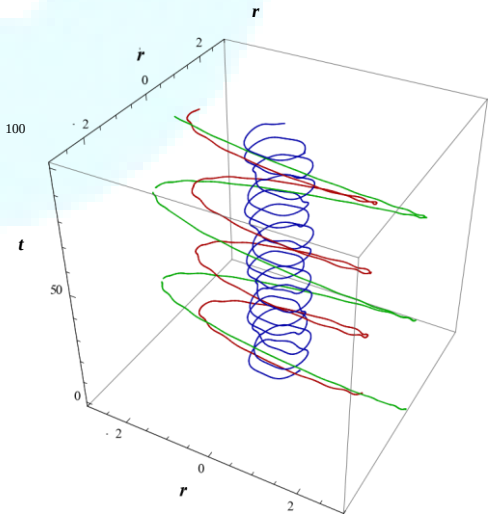

Figure 31: Trajectories for three identical ions with differing with differing initial radial positions.

$$m = 15 \quad U = 3 \quad V = 3 \quad \omega = 3.04 \quad r_0 = 0.5, 2.0, 3.0$$

While something of an extreme example, it's clear that depending on the distance between the electrodes, not all of the ions of a specified mass entering the quadrupole field will survive the journey to the other end. This kind of information would be extremely useful in the design of a quadrupole mass filter. Obviously, if ions were being eliminated unnecessarily then the instrument's sensitivity would be needlessly compromised. In this case, one solution would be to make sure that the distance between the rod electrodes was large enough so that even ions entering the

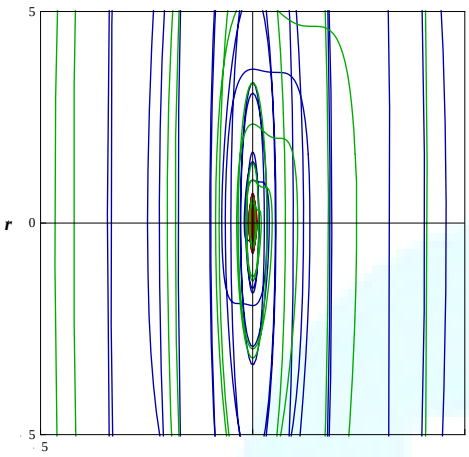

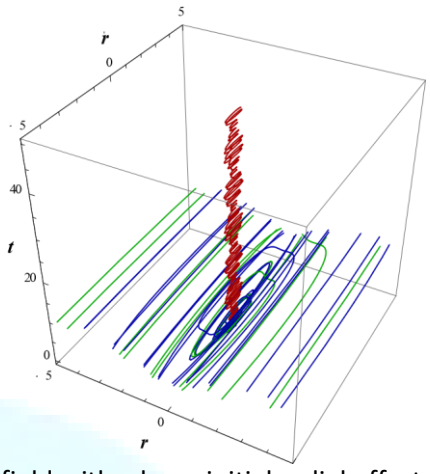

quadrupole field with a large initial radial offset was sufficient to accommodate their orbits. Alternatively, the radial offset of the ions entering the field could be reduced so that their orbital amplitudes were suitably small. This could be accomplished a number of ways, but using an ion lens to collimate the entering ions is one possibility.

Mass dependence:

Clearly the most important feature of a quadrupole mass filter is its ability to discriminate between ions of varying mass.

Once again, a plotting tool from the accompanying Mathematica file was employed to generate figures 32 and 33. These phase plots show the superimposed trajectories of three separate ions with differing masses subject to the same quadrupole field.

r_0 5

Figure 32: QMF in action!
Ions of mass 4 (blue), 5 (red) and 6 (green).

Figure 33: QMF in action! 5

Ions of mass 4 (blue), 5 (red) and 6 (green).

$$m = 4, 5, 6 \quad U = 3 \quad V = 3 \quad \omega = 3.24 \quad r_0 = 0.1$$

Even though the 2-D phase plot looks a bit messy (figure 32), it was surprisingly easy to find a set of parameters that demonstrate how the quadrupole field can be used as a mass filter. Only the middle mass (mass 5, the red trajectory) retains a stable trajectory through the field while the mass either side of it are ejected from the field due to their rapidly increasing orbit amplitudes.

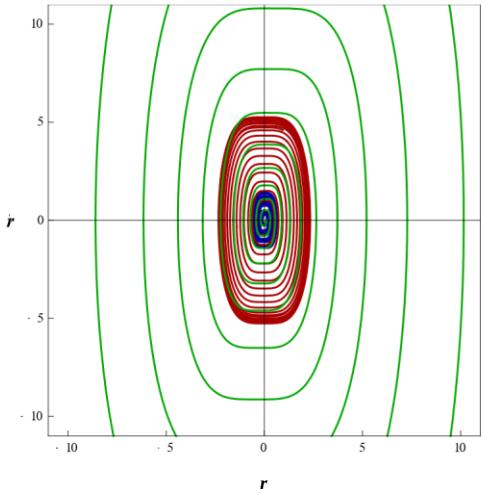

Figure 34: QMF in high-pass mode.

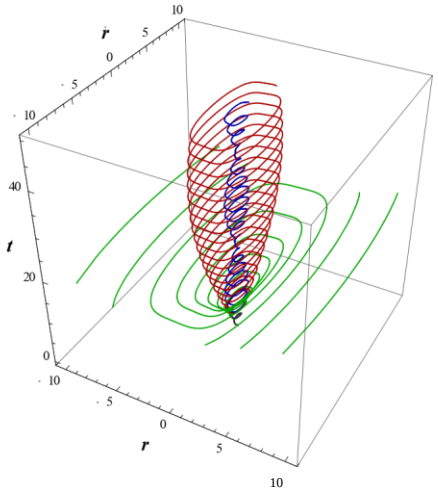

Figure 35: QMF in high-pass mode.

$$m = 66, 65, 64 \quad U = 3 \quad V = 3 \quad \omega = 5.30 \quad r_0 = 0.1$$

A far prettier pair of phase plots were produced (figures 34 and 35) by adjusting the quadrupole parameters so that mass 64 (green trajectory) would be ejected from the field, 65 (red trajectory) was just stable enough to pass through (depending on electrode separation of course) and mass 66 has a nice tight orbital trajectory.

These phase plots could easily be used by a person designing or modifying a quadrupole field-based instrument just as described earlier. Being able to determine the optimum electrode configuration, voltage parameters and range of initial ion positions would permit close matching to the intended application.